

Two-photon dissociation of BeH^+ with a middle ultraviolet band laser

Qian-Yu Zhang(张乾煜), Wen-Li Bai(白文丽), Zhi-Yuan Ao(敖致远), Wen-Cui Peng(彭文翠), Sheng-Guo He(何胜国), and Xin Tong(童昕)

Citation: Chin. Phys. B, 2025, 34 (**3**): 033301. DOI: 10.1088/1674-1056/ada436
Journal homepage: http://cpb.iphy.ac.cn; http://iopscience.iop.org/cpb

What follows is a list of articles you may be interested in

Computational design of ratiometric two-photon fluorescent Zn^{2+} probes based on quinoline and di-2-picolylamine moieties

Zhe Shao(邵哲), Wen-Ying Zhang(张纹莹), and Ke Zhao(赵珂)
Chin. Phys. B, 2022, 31 (**5**): 053302. DOI: 10.1088/1674-1056/ac46c6

Responsive mechanism and coordination mode effect of a bipyridine-based two-photon fluorescent probe for zinc ion

Han Zhang(张瀚), Zhe Shao(邵哲), Ke Zhao(赵珂)
Chin. Phys. B, 2020, 29 (**8**): 083304. DOI: 10.1088/1674-1056/aba9b9

Responsive mechanism and molecular design of di-2-picolylamine-based two-photon fluorescent probes for zinc ions

Mei-Yu Zhu(朱美玉), Ke Zhao(赵珂), Jun Song(宋军), Chuan-Kui Wang(王传奎)
Chin. Phys. B, 2018, 27 (**2**): 023302. DOI: 10.1088/1674-1056/27/2/023302

Time-dependent approach to the double-channel dissociation of the NaCs molecule induced by pulsed lasers

Zhang Cai-Xia (张彩霞), Niu Yu-Quan (牛余全), Meng Qing-Tian (孟庆田)
Chin. Phys. B, 2014, 23 (**10**): 103301. DOI: 10.1088/1674-1056/23/10/103301

Manifestation of external field effect in time-resolved photo-dissociation dynamics of LiF

Meng Qing-Tian (孟庆田), A. J. C. Varandas
Chin. Phys. B, 2013, 22 (**7**): 073303. DOI: 10.1088/1674-1056/22/7/073303

Two-photon dissociation of BeH^+ with a middle ultraviolet band laser

Qian-Yu Zhang(张乾煜)[1,2], Wen-Li Bai(白文丽)[1,2], Zhi-Yuan Ao(敖致远)[1,2], Wen-Cui Peng(彭文翠)[1], Sheng-Guo He(何胜国)[1,†], and Xin Tong(童昕)[1,3,‡]

[1] *State Key Laboratory of Magnetic Resonance and Atomic and Molecular Physics, Innovation Academy for Precision Measurement Science and Technology, Chinese Academy of Sciences, Wuhan* 430071, *China*
[2] *University of Chinese Academy of Sciences, Beijing* 100049, *China*
[3] *Wuhan Institute of Quantum Technology, Wuhan* 430206, *China*

(Received 16 December 2024; revised manuscript received 20 December 2024; accepted manuscript online 31 December 2024)

Two-photon dissociation of BeH^+ ions is studied by detecting the fluorescence changes of Be^+–BeH^+ bi-component Coulomb crystal in a linear Paul trap. BeH^+ ions generated by an exothermic reaction between electronically excited Be^+ ions and residual H_2 in the vacuum chamber are photon-dissociated with two photons scanning over the range of 201 nm to 208 nm. Our experiment provides a novel method to maintain the number of Be^+ ions stable in a Coulomb crystal with a middle ultraviolet band dissociation laser. This two-photon dissociation method extends the wavelength range of the dissociation laser for BeH^+ compared to the one-photon dissociation, and the method can be utilized to all alkaline earth atomic ions which require suppression of the reaction with residual H_2 gas in vacuum.

Keywords: photo-dissociation, two-photon absorption, chemical reaction, BeH^+

PACS: 33.80.Gj, 33.40.+f, 82.20.Kh, 82.30.Fi

DOI: 10.1088/1674-1056/ada436 **CSTR:** 32038.14.CPB.ada436

1. Introduction

Laser-cooled alkaline-earth atomic ions provide a strong foundation for quantum information processing,[1,2] quantum logic spectroscopy,[3,4] optical clocks,[5,6] and searching for the physics beyond the standard model.[7,8] However, previous studies have shown that these ions, particularly in their electronically-excited states, unavoidably react with residual H_2 gas in the vacuum chamber and the reaction rate is roughly proportional to the density of the reactant gas.[9–13] By placing the alkaline-earth ions in a cryogenic environment, where the residual background gas is greatly reduced, the reaction is suppressed and the chemical lifetime of ions is increased accordingly.[9,10] However, creating the cryogenic environment requires a complex apparatus, which may introduce additional noise from acoustic vibrations produced by the compression and expansion cycles of the cold head.[9] Alternatively, photo-dissociation (PD) of the hydride molecular ions such as BeH^+,[11] YbH^+,[12] and BaH^+,[13] has also been demonstrated to convert the reaction products back to atomic ions. Such approach relies on a dissociation laser with appropriate wavelength and energy, and the dynamics of photo-dissociation depends on the potential curves of the hydride molecular ions.

BeH^+ ions can be photo-dissociated by an ultraviolet (UV) range laser. Under thermal equilibrium, the photo-dissociation of BeH^+ at its vibrational ground state has been demonstrated using a 157-nm laser, and the dissociating rate of 1.3 ions per laser pulse has been achieved at the averaged pulse intensity of 21 $W\cdot cm^{-2}$.[11] The cutoff wavelength for the one-photon dissociation of BeH^+ in the vibrational ground state is calculated to be 177 nm. However, the difficulties associated with generating such short-wavelength lasers and their significant absorption by oxygen in the air limit the broad application of this method. An alternative way is to use two-photon processes for the dissociation of the hydride molecular ions. Two-photon dissociation has been achieved for the dissociation of CaH^+ molecular ion back into Ca^+ ion.[14] By scanning the dissociation laser wavelength from 370 nm to 420 nm, four resonance transitions from the vibrational $v = 0$ ground state to the $v' = 1$–4 excited states in CaH^+ were also observed.

In this article, a middle ultraviolet band laser is first utilized for two-photon dissociation of BeH^+ ions produced by the chemical reaction between laser-cooled Be^+ Coulomb crystal and H_2 molecules. The dissociation rate of BeH^+ is determined by the fluorescence changes of Be^+ Coulomb crystal. The suppressed fluorescence decay indicates the BeH^+ ions dissociating back to Be^+ ions, and this dissociation process can be utilized to stabilize the number of ions and the size of entire Be^+ ion-crystal. The resulting dissociation rates versus dissociation laser wavelength reveal the near resonance between the first absorbed photon and the corresponding transition of BeH^+ ions.

†Corresponding author. E-mail: hesg@wipm.ac.cn
‡Corresponding author. E-mail: tongxin@wipm.ac.cn

© 2025 Chinese Physical Society and IOP Publishing Ltd. All rights, including for text and data mining, AI training, and similar technologies, are reserved.

2. Experimental scheme

The illustration of experimental setup is shown in Fig. 1(a). A detailed description of the Be^+ ions crystal production can be found in our previous work.[15–17] Here, a brief introduction is provided. The Be atomic beam, produced by a Be oven, passes through the center of a linear Paul trap and is ionized through a $[2+1]$ resonance-enhanced multiphoton ionization process by a pulsed 306-nm photo-ionization (PI) laser. The produced Be^+ ions are trapped and then laser-cooled by two counter-propagating 313-nm laser beams along the trap axis, forming a Coulomb crystal in the trap. The fluorescence of the Be^+ ions, caused by spontaneous emission from the excited state $^2P_{3/2}$ to the ground state $^2S_{1/2}$, is detected by a CCD camera (see in Fig. 1(b)) and a photomultiplier tube (PMT). As demonstrated by molecular dynamic simulations in Ref. [18], the fluorescence of Be^+ ions exhibits a linear correlation to the number of Be^+ ions. Therefore, the relative number of Be^+ ions is evaluated by the Be^+ ions fluorescence collected by the PMT. The Be^+ Coulomb crystal is placed in a 300-K vacuum chamber. The background pressure of the chamber is 3×10^{-10} mbar (1 bar = 10^5 Pa), where the main component of residual gas is H_2 and the partial pressure of other components (H_2O, O_2, N_2, CO_2, etc.) is at least one order of magnitude lower. Therefore, the chemical reaction rate of Be^+ ions with other background gas, such as H_2O[19] and methanol,[11] is at least one order of magnitude lower than the reaction with H_2. Their influence on the fluorescence of Be^+ ions is negligible and not taken into account on the current experiment.

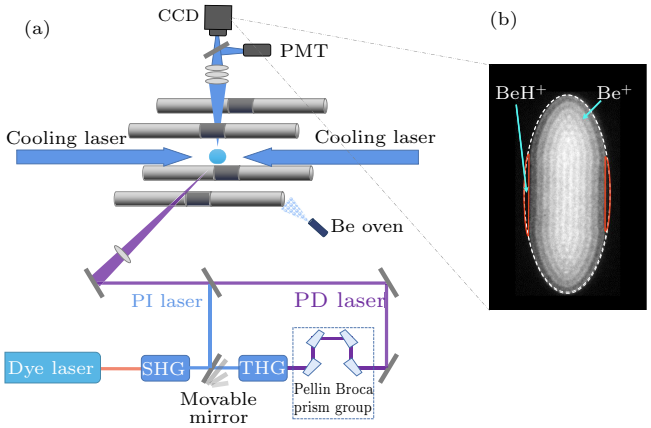


Fig. 1. Schematic diagram of the experimental setup: (a) illustration of the linear Paul trap and the setups of cooling laser, photo-ionization (PI) laser and photo-dissociation (PD) laser. The ellipsoidal Coulomb crystal of Be^+ ions at the center of the trap is detected by a CCD camera and a PMT. (b) An image of a Be^+–BeH^+ bi-component Coulomb crystal. The numbers of Be^+ and BeH^+ are about 2000 and 200, respectively. The area of the image captured by the CCD camera is 0.74 mm×0.48 mm. The white dashed line represents the boundary of the Coulomb crystal including the Be^+ ions and the BeH^+ ions. The orange solid line represents the boundary of the BeH^+ ions. This image is captured at hundreds of seconds after turning on the 208-nm dissociation laser, with the intensity of fluorescence and the size of Coulomb crystal remaining stable.

After the formation of the Be^+ Coulomb crystal, BeH^+ ions are generated through a chemical reaction between Be^+ ions and residual H_2 gas in the vacuum chamber. Since $Be^+(^2S) + H_2 \rightarrow BeH^+ + H$ is endothermic by 1.57 eV,[20] only Be^+ ions populated in the excited state ^2P due to the laser cooling react with H_2 gas. The BeH^+ ions are then sympathetically cooled by laser-cooled Be^+ ions to form a bi-component Be^+–BeH^+ Coulomb crystal. The contour line of bi-component Coulomb crystal remains the same as the pure Be^+ Coulomb crystal, indicating that the BeH^+ ions produced by the reaction are all trapped in the ion trap.

Both the photo-dissociation (PD) laser of BeH^+ ions and the photo-ionization (PI) laser of Be atoms are generated from the same dye laser (mixed dye type: 0.17-gram/liter Rh B and 0.04-gram/liter Rh 101), which is pumped by a 532-nm Nd:YAG laser at a repetition rate of 10 Hz and pulse width of 8 ns. The output of the dye laser can be tuned from 598 nm to 636 nm with a maximum conversion efficiency of about 16%. The output of the second harmonic generation (SHG) of the dye laser, diverted by a movable mirror, passes through the trap center and ionizes the Be atoms. The output of the third harmonic generation (THG) of the dye laser is extracted and focused on the trap center to dissociate the BeH^+ ions. The efficiency of the THG is about 5% with a β-BaB_2O_4 crystal. Four Pellin Broca prisms extract the output of THG laser and keep the beam path unchanged while scanning the PD laser wavelength from 201 nm to 208 nm. The peak intensity of the dissociation laser is 9×10^6 W·cm^{-2}, with a laser energy of 0.05-mJ per pulse and a beam diameter of 0.3 mm.

Figure 2 shows the potential curve of the lowest three spin-singlet electronic state of BeH^+ ion.[21–24] Considering the wavelength of the pulsed laser used in our experiment, there are three possible channels for dissociating BeH^+ into Be^+ and H. The channel one of a two-photon dissociation process (shown as a red arrow and labeled as CH1 in Fig. 2) indicates that BeH^+ ions in the vibrational ground state dissociate through the $BeH^+(X^1\Sigma^+) + 2h\nu \rightarrow BeH^+(A^1\Sigma^+) \rightarrow Be^+(^2P) + H(^1S)$ process with the wavelength of dissociation laser from 201 nm to 208 nm. In this channel, when the dissociation laser is near resonance to the vibrational states in $A^1\Sigma^+$ state, the dissociation rates can significantly increase.[14,25] The other two-photon dissociation channel (shown as a blue arrow and labeled as CH2 in Fig. 2) is that BeH^+ ions in the vibrational ground state are photon-dissociated via $BeH^+(X^1\Sigma^+) + 2h\nu \rightarrow BeH^+(B^1\Pi) \rightarrow Be^+(^2P) + H(^1S)$ by a 306-nm laser generated from the SHG of the dye laser. The channel three of a one-photon dissociation process (shown as a green arrow and labeled as CH3 in Fig. 2) is related to the dissociation of BeH^+ ions in the vibrational excited state via a $BeH^+(X^1\Sigma^+) + h\nu \rightarrow BeH^+(B^1\Pi) \rightarrow Be^+(^2P) + H(^1S)$ process with the dissociation laser ranging from 201 nm to

208 nm.

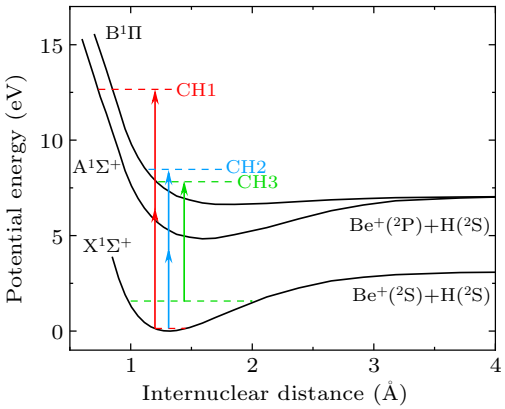


Fig. 2. Potential energy curves of the lowest three spin-singlet electronic states of BeH^+.[21–24] The red arrow and green arrow represent the dissociation process with the wavelength of dissociation laser from 201 nm to 208 nm labeled as CH1 and CH3, respectively. The blue arrow represents the dissociation process with the wavelength of dissociation laser at 306 nm labeled as CH2.

3. Results and discussion

The effect of the residual H_2 gas on the fluorescence of Be^+ ions is investigated in the first step. An initial Coulomb crystal of Be^+ ions is purified by changing endcap voltage of the ion trap to remove BeH^+ ions. Without the dissociation laser, shown as the blue line in Fig. 3(a), The fluorescence of Be^+ ions gradually disappears over 600 s. The decrease in fluorescence indicates a loss of Be^+ ions. The recorded fluorescence of Be^+ ions is fitted by a decay function, $y(t) = \exp(-Rt)$. The decay rate R is determined to be 0.006(1) s^{-1} from the fitting result of the recorded fluorescence. The decay rate of Be^+ ions R^* which caused by the reaction between Be^+ ions and H_2 can be evaluated by $R^* = k_L \alpha n$, where $k_L = 1.6 \times 10^{-9}$ $cm^3 \cdot s^{-1}$ is the Langevin rate constant of the reaction of Be^+ with H_2,[26] α is the population of Be^+ ions in the $^2P_{3/2}$ state, $n = 7(2) \times 10^6$ cm^{-3} is the number density of H_2. Here, we assume that the number density of H_2 remains constant during the reaction process. In our experiment, the intensity of the cooling laser is three times higher than the saturation intensity of 0.83 $mW \cdot mm^{-2}$. Therefore, the saturation parameter s is 3 and $\alpha \approx s/[2(s+1)] = 0.4$. Combined with the above parameters, the decay rate R^* is estimated to be 0.0045(13) s^{-1}, which is consistent with R obtained from fitting of the fluorescence signals. Thus, it confirms that the dominating loss channel of Be^+ ions is indeed due to the chemical reaction with H_2.

To investigate the photon dissociation process of BeH^+ ions, the fluorescence signal of the purified Be^+ crystal is recorded when the dissociation laser is turned on. The wavelength of the dissociation laser can be scanned from 201 nm to 208 nm with 1-nm step and the laser intensity remains the same. The fluorescence decay of Be^+ ions with a dissociation laser at 201 nm recorded over a consecutive period of 220 s is shown as the red line in Fig. 3(b). After 150 s, the fluorescence counts of Be^+ ions shown at point B in Fig. 3(b) decrease about 17% compared with the initial prepared pure Be^+ crystal at point A in Fig. 3(b). For the following tens of seconds as shown from the point B to point C, the fluorescence signals remain nearly constant and fluctuate within the range of 5%. Compared to the fluorescence decay without dissociation laser, the overall attenuation of the fluorescence of Be^+ ions is obviously suppressed due to photo-dissociation of the BeH^+ ions. The stabilization of Be^+ fluorescence after 150 s indicates the dynamic equilibrium between the regeneration of Be^+ by photo-dissociation and the reduction of Be^+ by chemical reaction. Similar to the fluorescence changes with the 201-nm laser turned on, the photo-dissociation of the BeH^+ ions is also observed when the dissociation laser is scanned from 201 nm to 208 nm. As shown by the green line in Fig. 3(a), the fluorescence of Be^+ ions with the dissociation laser at 208 nm decreases about 16% until the dynamic equilibrium is reached. The total reduction of fluorescence before reaching equilibrium exhibits slight variations, indicating the wavelength-dependent nature of the dissociation rate.

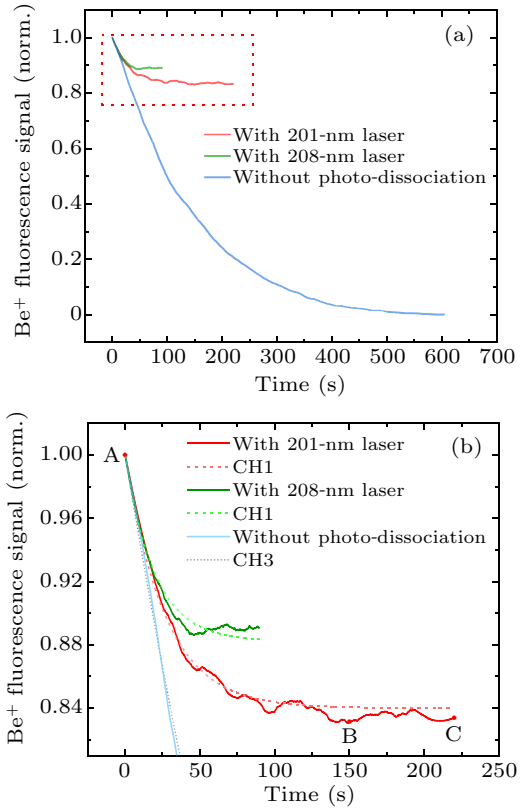


Fig. 3. The time evolution of Be^+ fluorescence recorded by PMT. (a) The blue solid line indicates the change of fluorescence counts without dissociation laser. The red solid and green solid lines are the change of fluorescence counts with 201-nm and 208-nm dissociation lasers, respectively. (b) An enlarged view of the rectangular area framed by red dotted lines in Fig. 3(a). The red and greens dash lines represent the influence of the dissociation through CH1 channel with 201-nm and 208-nm dissociation lasers, respectively. The grey dotted line represents the influence of the dissociation through CH3 channel.

By fitting the time evolution curve of the Be^+ ions flu-

orescence, the dissociation rate can be obtained. In thermal equilibrium of 300 K, less than 0.01% of BeH^+ ions populate vibrational excited states,[11] therefore, almost all the BeH^+ ions are photo-dissociated through the CH1 channel. The time evolution of the numbers of Be^+ ions and BeH^+ ions can be expressed as

$$\begin{cases} \partial N_{Be^+}(t)/\partial t = -RN_{Be^+}(t) + D(\lambda)N_{BeH^+}(t), \\ \partial N_{BeH^+}(t)/\partial t = RN_{Be^+}(t) - D(\lambda)N_{BeH^+}(t), \end{cases} \tag{1}$$

where $N_{Be^+}(t)$ and $N_{BeH+}(t)$ are the normalized (norm.) numbers of Be^+ ions and BeH^+ ions at time t, respectively, $R = 0.006(1)\ s^{-1}$ is the reaction rate of Be^+ with H_2, $D(\lambda)$ is the two-photon dissociation rate of BeH^+ ions with the dissociation laser at the given wavelength λ. The initial pure Be^+ crystal is prepared at $t = 0$, so that $N_{Be^+}(0)$ and $N_{BeH^+}(0)$ are 1 and 0, respectively. The number of Be^+ ions can then be derived as

$$N_{Be^+}(t) = \frac{D(\lambda)}{R+D(\lambda)} + \frac{R}{R+D(\lambda)} e^{-(R+D(\lambda))t}. \tag{2}$$

By fitting the time-varying fluorescence signals in Fig. 3(b) using Eq. (2), the dissociation rate with 201-nm laser and 208-nm laser are evaluated as 0.032(5) s^{-1} and 0.045(7) s^{-1}, respectively.

In addition to the dissociation of BeH^+ ions from the vibrational ground state, the dissociation from vibrational excited states is also needed to be considered. The dynamics calculations of the chemical reaction between Be^+ and H_2[27] has been implemented using the time-dependent wave packet (TDWP) method. These calculations reveal that the vibrational quantum number v of the product BeH^+ molecular ions ranges from 0 to 10. For the dissociation laser wavelength ranging from 201 nm to 208 nm, BeH^+ ions in the v =0 vibrational state cannot be one-photon dissociated due to the energetic reason. While BeH^+ ions in the vibrational excited states may undergo one-photon dissociation[28] before they decay to the vibrational ground state. To include the dissociation of BeH^+ ions from the vibrational excited states ($v = 1, 2, \ldots, 10$) by a single photon (CH3 in Fig. 2), the time evolution equations for the numbers of Be^+ and BeH^+ ions are modified as follows:

$$\begin{cases} \partial N_{Be^+}(t)/\partial t = -RN_{Be^+}(t) + \sum_{v=1}^{10} D_v(\lambda)N_v(t), \\ \partial N_v(t)/\partial t = n_v RN_{Be^+}(t) - D_v(\lambda)N_v(t) - A_v N_v(t) + A_{v+1}N_{v+1}(t), \quad v = 1, \ldots, 10, \end{cases} \tag{3}$$

where N_v is the number of BeH^+ ions with vibrational quantum number v from 1 to 10, $D_v(\lambda)$ is the one-photon dissociation rate calculated in Ref. [28], n_v is the population of the v-th vibrational excited state of the BeH^+ ions produced by the chemical reaction calculated in Ref. [27], A_v is the spontaneous emission rate of the vibrational state v in Ref. [29]. In Eq. (3), spontaneous emission between adjacent vibrational states is only considered, and rotational excited states with higher spontaneous emission rates and BBR effect are not included. The above approximate conditions may result in underestimated decay rate and overestimated population of the vibrational excited states. Therefore, the dissociation process via CH3 channel may also be overestimated. The number of Be^+ ions, obtained by solving the time-dependent Eq. (3), is shown in Fig. 3(b) as the grey dotted line. The consistency among the calculated results and the time evolution of fluorescence without dissociation laser suggests that the CH3 channel has little contribution to the dissociation of BeH^+ even under the approximate conditions which exaggerate the dissociation process. The reason for this is that, given the laser intensity employed in this experiment, the dissociation rates of the vibrational excited states ($\sim 1\ s^{-1}$) are significantly lower compared to the rate of spontaneous emission ($\sim 10\ s^{-1}$). Therefore, the dissociation of BeH^+ ions in our experiment is dominated by two-photon dissociation of BeH^+ ions in the vibrational ground state (CH1 channel). The time-dependent number of Be^+ ions can be appropriately described by Eq. (2).

For the two-photon dissociation of BeH^+ ions with the laser scanning from 201 nm to 208 nm, the dissociation rates are obtained by fitting the Be^+ fluorescence using Eq. (2) when the PD laser is scanned. Then the two-photon dissociation cross-sections $\sigma(\lambda)$ can be expressed as

$$\sigma(\lambda) = \frac{h^2c^2}{\tau f I^2 \lambda^2} D(\lambda), \tag{4}$$

where λ, τ, f, I are the wavelength, the pulse width, the repetition rate, and the peak intensity of the dissociation laser, respectively. h and c are the Planck constant and the speed of light in vacuum, respectively. Therefore, combing the measured dissociation rates and the parameters of the dissociation laser mentioned above, the $\sigma(\lambda)$ are obtained to be on the order of 10^{-45} $cm^4 \cdot s$ and increase monotonically from 201 nm to 208 nm as shown in Fig. 4. In our experiment, no resonance peaks were observed when the laser wavelength was scanned from 201 nm to 208 nm. This range covers the $X^1\Sigma^+$ ($v = 0$)–$A^1\Sigma^+$ ($v' = 7, 8$) transitions, as stated in the energy levels calculation of BeH^+ in Ref. [20]. In that reference, the Frank–Condon factors for the transitions $X^1\Sigma^+$ ($v = 0$)–$A^1\Sigma^+$ ($v' = 0, 1, 2, 3, 4$) were also calculated as 0.14, 0.23, 0.22,

0.17, 0.11, respectively. The overtone transitions of $X^1\Sigma^+$ ($v = 0$)–$A^1\Sigma^+$ ($v' = 7$, 8) are rather weak. The observed increase of the two-photon dissociation cross-section as the dissociation laser wavelength scanned from 201 nm to 208 nm is presumably due to certain lower overtone vibrational transitions with resonance peaks beyond 208 nm.

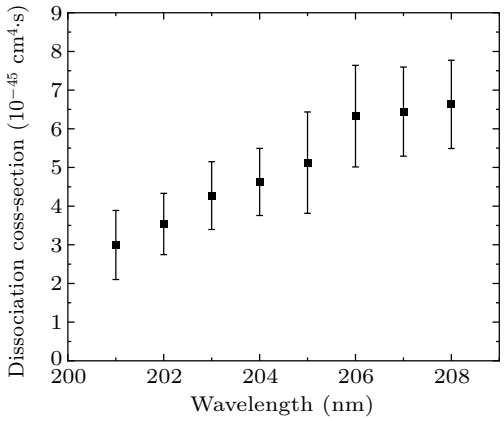


Fig. 4. The two-photon dissociation cross-section *versus* the wavelength of dissociation laser. The black squares are corresponding to experimental data which is the average of five experimental measurements.

In our experiment, the two-photon dissociation of BeH^+ ions through the CH2 channel is also observed when the wavelength of the dissociation laser is set to 306 nm. The measured dissociation rate is 0.050(9) s^{-1} with laser energy of 3-mJ per pulse. Using Eq. (4), the two-photon dissociation cross-section at 306 nm is calculated to be $2.8(6)\times10^{-48}$ cm^4·s. This value is three orders of magnitude lower than the two-photon dissociation cross-section of CH1. The higher two-photon dissociation cross-section of CH1 may suggest that the first absorption photon with the laser wavelength from 201 nm to 208 nm is near resonant with vibrational states in the $A^1\Sigma^+$ state as indicated in Fig. 2.

4. Conclusion

In summary, the two-photon dissociation of BeH^+ ions in the middle ultraviolet spectral range is demonstrated. The dissociating rate of 0.03 to 0.05 ions per second is achieved at an averaged pulse intensity of 0.72 W·cm^{-2}. The fluorescence of Be^+ ions reaches stable condition due to the dynamic equilibrium between the chemical reaction of $Be^+ + H_2$ and photodissociation of the reactional product BeH^+ ions. Such stable condition of the fluorescence from the laser-cooled Be^+ ions is helpful for the experiments relying on Be^+ Coulomb crystal, such as our previous work detecting rovibrational transition of HD^+.[30,31] Our two-photon dissociation scheme extends the wavelength of the dissociation laser of BeH^+ to the range of 201 nm to 208 nm. The two-photon dissociation method can be applied to all alkaline earth atomic ions that require suppression of the reaction with residual H_2 gas. Compared to one-photon dissociation, the two-photon dissociation scheme demands a dissociation laser with a longer wavelength within the mid-UV range, which is relatively more obtainable and economical to procure. Our work also suggests a possibility of covering the wavelength range for dissociating both BeH^+ and $BeOH^+$ ions with a single laser beam.[13] Such an accomplishment was regarded as unfeasible in Ref. [13], where only one-photon dissociation is involved. The two-photon dissociation of BeH^+ can be achieved to measure the vibronic spectroscopy of $X^1\Sigma^+$–$A^1\Sigma^+$ transition.[21] This resonant dissociation can also be provided to distinguish the isotopes between BeH^+ and BeD^+ for studying the reaction dynamics between Be^+ and HD.[26] Additionally, there is currently a lack of theoretical calculations for two-photon dissociation cross-sections. Our next move will be to acquire the full $X^1\Sigma^+$–$A^1\Sigma^+$ vibrational band spectroscopy of BeH^+ and perform theoretical calculations for verification, including both vibrational constants and dissociation cross-sections.

Acknowledgements

We thank Yukun Yang and Songbin Zhang for providing calculation results of the photo-dissociation cross sections of BeH^+. We also appreciate Maodu Chen for providing supports for calculating the population of rovibrational states of BeH^+ produced by chemical reaction between Be^+ and H_2.

Project supported by the National Key Research and Development Program of China (Grant No. 2021YFA1402103) and the National Natural Science Foundation of China (Grant No. 12393825).

References

[1] Christensen J E, Hucul D, Campbell W C and Hudson E R 2020 *Npj Quantum Inf.* **6** 35
[2] Srinivas R, Burd S C, Knaack H M, Sutherland R T, Kwiatkowski A, Glancy S, Knill E, Wineland D J, Leibfried D, Wilson A C, Allcock D T C and Slichter D H 2021 *Nature* **597** 209
[3] Schmidt P O, Rosenband T, Langer C, Itano W M, Bergquist J C and Wineland D J 2005 *Science* **309** 749
[4] Micke P, Leopold T, King S A, Benkler E, Spieß L J, Schmöger L, Schwarz M, Crespo López-Urrutia J R and Schmidt P O 2020 *Nature* **578** 60
[5] Huang Y, Guan H, Zeng M, Tang L and Gao K 2019 *Phys. Rev. A* **99** 011401
[6] Dörscher S, Huntemann N, Schwarz R, Lange R, Benkler E, Lipphardt B, Sterr U, Peik E and Lisdat C 2021 *Metrologia* **58** 015005
[7] Hur J, Aude Craik D P L, Counts I, Knyazev E A, Caldwell L, Leung C, Pandey S, Berengut J C, Geddes A J, Nazarewicz W, Reinhard P G, Kawasaki A, Jeon H, Jhe W and Vuletić V 2022 *Phys. Rev. Lett.* **128** 163201
[8] Alighanbari S, Kortunov I V, Giri G S and Schiller S 2023 *Nat. Phys.* **19** 1263
[9] Pagano G, Hess P W, Kaplan H B, Tan W L, Richerme P, Becker P, Kyprianidis A, Zhang J, Birckelbaw E, Hernandez M R, Wu Y and Monroe C 2019 *Quantum Sci. Technol.* **4** 014004
[10] Leopold T, King S A, Micke P, Bautista-Salvador A, Heip J C, Ospelkaus C, Crespo Løpez-Urrutia J R and Schmidt P O 2019 *Rev. Sci. Instrum.* **90** 073201
[11] Sawyer B C, Bohnet J G, Britton J W and Bollinger J J 2014 *Phys. Rev. A* **91** 011401

[12] Hoang T M, Jau Y Y, Overstreet R and Schwindt P D D 2020 *Phys. Rev. A* **101** 022705
[13] Wu H, Mills M, West E, Heaven M C and Hudson E R 2021 *Phys. Rev. A* **104** 063103
[14] Rugango R, Calvin A T, Janardan S, Shu G and Brown K R 2016 *ChemPhysChem* **17** 3764
[15] Li M, Zhang Y, Zhang Q Y, Bai W L, He S G, Peng W C and Tong X 2022 *J. Phys. B: At. Mol. Opt. Phys.* **55** 035002
[16] Li H X, Li M, Zhang Q Y and Tong X 2019 *Chin. Phys. Lett.* **36** 073701
[17] Li M, Zhang Y, Zhang Q Y, Bai W L, He S G, Peng W C and Tong X 2023 *Chin. Phys. B* **32** 036402
[18] Zhang Y, Zhang Q Y, Bai W L, Peng W C, He S G and Tong X 2023 *Chin. J. Phys.* **84** 164
[19] Yang T, Li A, Chen G K, Xie C, Suits A G, Campbell W C, Guo H and Hudson E R 2018 *J. Phys. Chem. Lett.* **9** 3555
[20] Raimondi M and Gerratt J 1983 *J. Chem. Phys.* **79** 4339
[21] Machado F B C and Ornellas F R 1991 *J. Chem. Phys.* **94** 7237
[22] Farjallah M, Ghanmi C and Berriche H 2013 *Eur. Phys. J. D* **67** 245
[23] Wan M, Wang F and Cao Q 2014 *Mol. Phys.* **112** 2184
[24] Xu X S, Dai A Q, Peng Y G, Wu Y and Wang J G 2018 *J. Quantum Spectrosc. Radiat. Transfer* **206** 172
[25] Højbjerre K, Hansen A K, Skyt P S, Staanum P F and Drewsen M 2009 *New J. Phys.* **11** 055026
[26] Roth B, Blythe P, Wenz H, Daerr H and Schiller S 2006 *Phys. Rev. A* **73** 042712
[27] Yang Z, Yuan J, Wang S and Chen M 2018 *RSC Adv.* **8** 22823
[28] Yang Y K, Cheng Y J, Peng Y G, Wu Y, Wang J G, Qu Y Z and Zhang S B 2020 *J. Quantum Spectrosc. Radiat. Transfer* **254** 107203
[29] Ornellas F R, Stwalley W C and Zemke W T 1983 *J. Chem. Phys.* **79** 5311
[30] Zhang Y, Zhang Q Y, Bai W L, Ao Z Y, Peng W C, He S G and Tong X 2023 *Phys. Rev. A* **107** 043101
[31] Zhang Q Y, Bai W L, Ao Z Y, Ding Y H, Peng W C, He S G and Tong X 2024 *Acta Phys. Sin.* **73** 203301 (in Chinese)